Input Estimation for Nonminimum-Phase Systems With Application to Acceleration Estimation for a Maneuvering Vehicle

Ahmad Ansari and Dennis S. Bernstein, *Fellow, IEEE*

***Abstract*— The goal of state and input estimation is to simultaneously estimate both the unmeasured states and unknown input. Although this problem has been widely studied, existing techniques are confined to the case where the system is minimum phase. This paper introduces retrospective cost input estimation (RCIE), which is based on retrospective cost optimization. It is shown that RCIE automatically develops an internal model of the unknown input. This internal model provides an asymptotic estimate of the unknown input regardless of the location of the zeros of the plant, including the case of nonminimum-phase (NMP) dynamics. RCIE is applied to the NMP problem of estimating inertial acceleration of a maneuvering unmanned aerial vehicle using optical position data.**

***Index Terms*— Input estimation, Kalman filter, maneuvering target tracking, nonminimum-phase (NMP) zeros.**

I. Introduction

THE Kalman filter and its variants provide well-established techniques for estimating states that are not directly measured [1]–[5]. The goal of these techniques is to obtain optimal state estimates in the presence of process and sensor noise. These techniques typically assume that the sensor and process noise are stationary with zero mean. If, however, the process noise includes a known deterministic component, then estimator bias can be avoided by injecting this component into the estimator; this technique underlies the separation principle of linear-quadratic-Gaussian control. If, however, the process noise is biased, that is, has unknown, nonzero mean, or, more generally, it includes an unknown deterministic component, then it is of interest to obtain estimates that are unbiased, that is, unaffected by the deterministic-but-unknown input. This problem is addressed in [6]–[10].

The advantages of injecting the known deterministic input signal into the estimator motivate the development of techniques for estimating not only the unmeasured states but also the unknown deterministic input. The value of this objective in practice resides in the fact that knowledge of the deterministic input and its injection into the estimator can greatly increase the accuracy of the state estimates relative to the *ad hoc* technique of choosing the disturbance covariance matrix to overbound the deterministic input. The potential value of this approach is evident from the increasing literature on input estimation [11]–[34].

An alternative approach to input estimation is to assume that the unknown input is the output of an auxiliary linear/nonlinear system with known dynamics driven by white noise. The dynamics of the auxiliary system are appended to the dynamics of the physical system, and the augmented model is used as the basis of the state estimator [35]–[37]. This approach may not be accurate, however, if the unknown input cannot be approximated by the output of a linear system driven by white noise. The approach of this paper can be viewed as an adaptive technique for learning suitable dynamics that capture the unknown input.

The motivation for this paper resides in the fact that most of the techniques for state and input estimation cited above are confined to minimum-phase systems, that is, systems with invariant zeros contained in the open unit disk. In particular, the approach of [30], which extends the method of [16], explicitly invokes a minimum-phase assumption.

The case of nonminimum-phase (NMP) zeros, that is, zeros that are either on the unit circle or outside the closed unit disk, is much more challenging. As shown in [24], a naive attempt to estimate the input for an NMP system with zeros outside the closed unit disk yields a reconstruction error that is unbounded; in the case of zeros on the unit circle, the input-reconstruction error is bounded but nonzero. In contrast, in the case of MP systems, the input-reconstruction error vanishes asymptotically. Unlike most of the references cited above, [34] considers the case of NMP zeros, but the method is not applicable to the case of zeros on the unit circle.

More generally, it is important to stress that exact input reconstruction for a system with *any* zeros is impossible. This can be easily seen by noting that the presence of an invariant zero implies the existence of an initial condition and input for which the output is identically zero. These details are related to the *unobservable input subspace* [24]. Hence, in the case where the system has one or more invariant zeros, the goal is to achieve asymptotic input reconstruction of the component of the input that resides in the orthogonal complement of the unobservable input subspace.

This paper is aimed at the case where the system is NMP. In particular, this paper considers state and input estimation based on retrospective cost optimization [33], [38]–[43].

Manuscript received August 14, 2017; revised December 12, 2017; accepted February 2, 2018. Manuscript received in final form February 14, 2018. This work was supported by the Office of Naval Research under Grant N00014-14-1-0596. Recommended by Associate Editor H. Gao. *(Corresponding author: Ahmad Ansari.)*

The authors are with the Department of Aerospace Engineering, The University of Michigan, Ann Arbor, MI 48109 USA (e-mail: ansahmad@umich.edu; dsbaero@umich.edu).

Color versions of one or more of the figures in this paper are available online at http://ieeexplore.ieee.org.

Digital Object Identifier 10.1109/TCST.2018.2807798

Based on this technique, the contribution of this paper is the development of retrospective cost input estimation (RCIE), which is a technique for state and input estimation that is effective for NMP systems. This approach uses an estimator whose coefficients are recursively updated at each time step so as to minimize a retrospective cost function. Motivation for this approach is discussed within the context of adaptive control in [44] and [45].

The method developed in this paper provides a novel approach to a longstanding problem in target tracking, namely, estimation of the inertial acceleration of a body using only position measurements. This problem is motivated by the need to estimate acceleration in order to predict future motion and distinguish ballistic vehicles from maneuvering vehicles. The extensive literature and diverse methods developed for this problem attest to its importance [20], [39], [46]–[51]. It turns out that, for this problem, the discretized kinematics have invariant zeros on the unit circle, and thus the approach of [34] is not applicable. A more restricted version of RCIE confined to LTI systems is applied to this problem for planar target tracking in [41]. The approach of [41], however, is not applicable to LTV systems, such as the kinematics of a 3-D maneuvering vehicle resolved in the body frame. In addition, [41] does not recognize or address the NMP features of the problem.

The contents of this paper are as follows. Section II introduces the state and input estimation problem along with the RCIE algorithm and details of the input-estimation subsystem. Section III shows how RCIE can asymptotically reconstruct the input to an NMP system by embedding an internal model of the unknown input in the input-estimation subsystem. Section IV illustrates the effect of the unobservable input subspace, and Section V compares RCIE to the filter presented in [30]. Section VI provides the main objective of this paper, namely, application of RCIE to estimation of inertial acceleration. Using optical position data for an unmanned aerial vehicle (UAV), RCIE estimates the inertial acceleration, which is modeled as an unknown input. The acceleration estimates are compared with IMU data from onboard sensors.

II. Input and State Estimation

Consider the linear discrete-time system

$$\begin{aligned} x(k) = {} & A(k-1)x(k-1) + B(k-1)u(k-1) \\ & + G(k-1)d(k-1) + D_1(k-1)w(k-1) \qquad (1) \\ y(k) = {} & C(k)x(k) + D_2(k)v(k) \qquad (2) \end{aligned}$$

where $x(k) \in \mathbb{R}^{l_x}$ is the unknown state, $u(k) \in \mathbb{R}^{l_u}$ is the known input, $d(k) \in \mathbb{R}^{l_d}$ is the unknown input, $w(k) \in \mathbb{R}^{l_w}$ is the unknown white process noise with zero mean and unit variance, $y(k) \in \mathbb{R}^{l_y}$ is the measured output, and $v(k) \in \mathbb{R}^{l_v}$ is the unknown white measurement noise with zero mean and unit variance. This model may represent a sampled-data version of a continuous-time plant with sample time T_s, in which case $x(k)$ denotes the state at time $t = kT_s$. The matrices $A(k) \in \mathbb{R}^{l_x \times l_x}$, $B(k) \in \mathbb{R}^{l_x \times l_u}$, $G(k) \in \mathbb{R}^{l_x \times l_d}$, $D_1(k) \in \mathbb{R}^{l_x \times l_w}$, $C(k) \in \mathbb{R}^{l_y \times l_x}$, and $D_2(k) \in \mathbb{R}^{l_y \times l_v}$ are assumed to be known. The process noise covariance is $V_1(k) \triangleq D_1(k)D_1(k)^T \in \mathbb{R}^{l_x \times l_x}$, and the measurement noise covariance is $V_2(k) \triangleq D_2(k)D_2(k)^T \in \mathbb{R}^{l_y \times l_y}$. The goal is to estimate the unknown input $d(k)$ and the unknown state $x(k)$.

A. Retrospective Cost Input Estimation

In order to estimate the unknown input $d(k)$, we consider the Kalman filter forecast step

$$\begin{aligned} x_{fc}(k) = {} & A(k-1)x_{da}(k-1) + B(k-1)u(k-1) \\ & + G(k-1)\hat{d}(k-1) \qquad (3) \\ y_{fc}(k) = {} & C(k)x_{fc}(k) \qquad (4) \\ z(k) = {} & y_{fc}(k) - y(k) \qquad (5) \end{aligned}$$

where $\hat{d}(k) \in \mathbb{R}^{l_d}$ is the input estimate, $x_{da}(k) \in \mathbb{R}^{l_x}$ is the data-assimilation state, $x_{fc}(k) \in \mathbb{R}^{l_x}$ is the forecast state, and $z(k) \in \mathbb{R}^{l_y}$ is the innovations. The goal is to develop an input estimator that minimizes $z(k)$ by estimating $d(k)$.

We obtain the input estimate $\hat{d}(k)$ as the output of the *input-estimation subsystem* of order n_c given by

$$\hat{d}(k) = \sum_{i=1}^{n_c} P_i(k)\hat{d}(k-i) + \sum_{i=0}^{n_c} Q_i(k)z(k-i) \qquad (6)$$

where $P_i(k) \in \mathbb{R}^{l_d \times l_d}$ and $Q_i(k) \in \mathbb{R}^{l_d \times l_y}$. Note that (6) represents an exactly proper transfer function with direct feedthrough from the innovations $z(k)$ to the estimate $\hat{d}(k)$ of $d(k)$. RCIE minimizes $z(k)$ by updating $P_i(k)$ and $Q_i(k)$. The subsystem (6) can be reformulated as

$$\hat{d}(k) = \Phi(k)\theta(k) \qquad (7)$$

where the regressor matrix $\Phi(k)$ is defined by

$$\Phi(k) \triangleq \begin{bmatrix} \hat{d}(k-1) \\ \vdots \\ \hat{d}(k-n_c) \\ z(k) \\ \vdots \\ z(k-n_c) \end{bmatrix}^T \otimes I_{l_d} \in \mathbb{R}^{l_d \times l_\theta}$$

and

$$\theta(k) \triangleq \mathrm{vec}[P_1(k) \cdots P_{n_c}(k) \;\; Q_0(k) \cdots Q_{n_c}(k)] \in \mathbb{R}^{l_\theta},$$

where $l_\theta \triangleq l_d^2 n_c + l_d l_y (n_c + 1)$, "$\otimes$" is the Kronecker product, and "vec" is the column-stacking operator. The order n_c of the input-estimation subsystem must be chosen large enough to accommodate an internal model of the unknown input. The action of the internal model is described in Section III.

Define $l_y \times l_d$ filter $G_{f,k}(\mathbf{q}) \triangleq D_{f,k}^{-1}(\mathbf{q})N_{f,k}(\mathbf{q})$, where $\mathbf{q}$ is the forward shift operator, $n_f \geq 1$ is the order of G_f,

$$N_{f,k}(\mathbf{q}) \triangleq K_1(k)\mathbf{q}^{n_f-1} + K_2(k)\mathbf{q}^{n_f-2} + \cdots + K_{n_f}(k) \qquad (8)$$

$$D_{f,k}(\mathbf{q}) \triangleq I_{l_y}\mathbf{q}^{n_f} + A_1(k)\mathbf{q}^{n_f-1} + A_2(k)\mathbf{q}^{n_f-2} + \cdots + A_{n_f}(k) \qquad (9)$$

and, for all $1 \leq i \leq n_f$ and $k \geq 0$, $K_i(k) \in \mathbb{R}^{l_y \times l_d}$ and $A_i(k) \in \mathbb{R}^{l_y \times l_y}$.

Next, for all $k \geq 0$, we define the *retrospective input*

$$d_{rc}(\hat{\theta}, k) \triangleq \Phi(k)\hat{\theta} \tag{10}$$

and the corresponding *retrospective performance variable*

$$z_{rc}(\hat{\theta}, k) \triangleq z(k) + G_{f,k}(\mathbf{q})[d_{rc}(\hat{\theta}, k) - \hat{d}(k)] \tag{11}$$

where the filter $G_{f,k}(\mathbf{q})$ is derived in Section II-C and the coefficient vector $\hat{\theta} \in \mathbb{R}^{l_\theta}$ is determined by the following optimization. Defining

$$\Phi_f(k) \triangleq G_{f,k}(\mathbf{q})\Phi(k) \in \mathbb{R}^{l_y \times l_\theta} \tag{12}$$

$$\hat{d}_f(k) \triangleq G_{f,k}(\mathbf{q})\hat{d}(k) \in \mathbb{R}^{l_y} \tag{13}$$

it follows that $z_{rc}(\hat{\theta}, k)$ can be written as:

$$z_{rc}(\hat{\theta}, k) = z(k) + \Phi_f(k)\hat{\theta} - \hat{d}_f(k). \tag{14}$$

For $k \geq 1$, we define the retrospective cost function

$$J(\hat{\theta}, k) \triangleq \sum_{i=0}^{k} \lambda^{k-i}(z_{rc}(\hat{\theta}, i)^T R_z z_{rc}(\hat{\theta}, i) + [\Phi(i)\hat{\theta}]^T R_d \Phi(i)\hat{\theta}) + \lambda^k[\hat{\theta} - \theta(0)]^T R_\theta[\hat{\theta} - \theta(0)] \tag{15}$$

where $R_z \in \mathbb{R}^{l_y \times l_y}$, $R_d \in \mathbb{R}^{l_d \times l_d}$, and $R_\theta \in \mathbb{R}^{l_\theta \times l_\theta}$ are positive definite, and $\lambda \in (0, 1]$ is the forgetting factor. Let $P(0) = R_\theta^{-1}$ and $\theta(0) = \theta_0$. Then, for all $k \geq 1$, the cumulative cost function (15) has the unique global minimizer $\theta(k)$ given by the recursive least squares (RLS) update

$$\theta(k) = \theta(k-1) - P(k-1)\tilde{\Phi}(k)^T \Gamma(k)[\tilde{\Phi}(k)\theta(k-1) + \tilde{z}(k)] \tag{16}$$

$$P(k) = \frac{1}{\lambda}[P(k-1) - P(k-1)\tilde{\Phi}(k)^T \Gamma(k)\tilde{\Phi}(k)P(k-1)] \tag{17}$$

where

$$\tilde{\Phi}(k) \triangleq \begin{bmatrix} \Phi_f(k) \\ \Phi(k) \end{bmatrix} \in \mathbb{R}^{(l_y+l_d)\times l_\theta} \tag{18}$$

$$\tilde{R}(k) \triangleq \begin{bmatrix} R_z(k) & 0 \\ 0 & R_d(k) \end{bmatrix} \in \mathbb{R}^{(l_y+l_d)\times(l_y+l_d)} \tag{19}$$

$$\tilde{z}(k) \triangleq \begin{bmatrix} z(k) - \hat{d}_f(k) \\ 0 \end{bmatrix} \in \mathbb{R}^{l_y+l_d} \tag{20}$$

$$\Gamma(k) \triangleq [\lambda \tilde{R}(k)^{-1} + \tilde{\Phi}(k)P(k-1)\tilde{\Phi}(k)^T]^{-1}. \tag{21}$$

Note that RCIE uses RLS to estimate the coefficients θ of the input-estimation subsystem. Since the RLS equation is a quadratic matrix equation, its computational complexity is $O(n_c^2)$.

B. State Estimation

In order to estimate the state $x(k)$, we use $x_{fc}(k)$ given by (3) to obtain the estimate $x_{da}(k)$ of $x(k)$ given by the Kalman filter data-assimilation step

$$x_{da}(k) = x_{fc}(k) + K_{da}(k)z(k) \tag{22}$$

where the state estimator gain $K_{da}(k) \in \mathbb{R}^{l_x \times l_y}$ is given by

$$K_{da}(k) = -P_f(k)C(k)^T[C(k)P_f(k)C(k)^T + V_2(k)]^{-1} \tag{23}$$

and the forecast error covariance $P_f(k) \in \mathbb{R}^{l_x \times l_x}$ and the data-assimilation error covariance $P_{da}(k) \in \mathbb{R}^{l_x \times l_x}$ are given by

$$P_f(k) = A(k-1)P_{da}(k-1)A(k-1)^T + V_1(k-1) + V_{\hat{d}}(k-1) \tag{24}$$

$$P_{da}(k) = [I + K_{da}(k)C(k)]P_f(k) \tag{25}$$

where $V_{\hat{d}}(k)$ is the covariance of $\hat{d}(k)$. Note that, if $\hat{d}(k) = d(k)$ for all $k \geq 0$, then, for all $k \geq 0$, $V_{\hat{d}}(k) = 0$ and the state estimate x_{da} given by (22) is the standard Kalman filter estimate.

C. Filter Construction

For simplicity of presentation, the known input u and the process noise w are omitted in this section. By substituting (3) into (22), the forecast step is given as

$$x_{fc}(k) = \bar{A}(k-1)x_{fc}(k-1) + G(k-1)\hat{d}(k-1) + \bar{B}(k-1)y(k-1) \tag{26}$$

where

$$\bar{A}(k) \triangleq A(k)[I + K_{da}(k)C(k)], \quad \bar{B}(k) \triangleq -A(k)K_{da}(k). \tag{27}$$

The forecast state estimate $x_{fc}(k)$ given by (26) can be expanded as

$$\begin{aligned} x_{fc}(k) &= \left(\prod_{i=1}^{n} \bar{A}(k-i)\right) x_{fc}(k-n) \\ &\quad + \sum_{i=2}^{n} \left(\prod_{j=1}^{i-1} \bar{A}(k-j)\right) G(k-i)\hat{d}(k-i) + G(k-1)\hat{d}(k-1) \\ &\quad + \sum_{i=2}^{n} \left(\prod_{j=1}^{i-1} \bar{A}(k-j)\right) \bar{B}(k-i)y(k-i) + \bar{B}(k-1)y(k-1) \end{aligned} \tag{28}$$

where $\prod_{i=1}^{2} M_i \triangleq M_2 M_1$. Using (4) and (28) yields

$$z(k) = C(k)\left(\prod_{i=1}^{n} \bar{A}(k-i)\right) x_{fc}(k-n) + \sum_{i=1}^{n} H_i(k)\hat{d}(k-i) + \sum_{i=1}^{n} H_i'(k)y(k-i) - y(k) \tag{29}$$

where, for all $i \geq 1$

$$H_i(k) \triangleq \begin{cases} C(k)G(k-1), & i = 1 \\ C(k)\left(\prod_{j=1}^{i-1} \bar{A}(k-j)\right) G(k-i), & i \geq 2 \end{cases} \tag{30}$$

$$H_i'(k) \triangleq \begin{cases} C(k)\bar{B}(k-1), & i = 1 \\ C(k)\left(\prod_{j=1}^{i-1} \bar{A}(k-j)\right) \bar{B}(k-i), & i \geq 2. \end{cases} \tag{31}$$

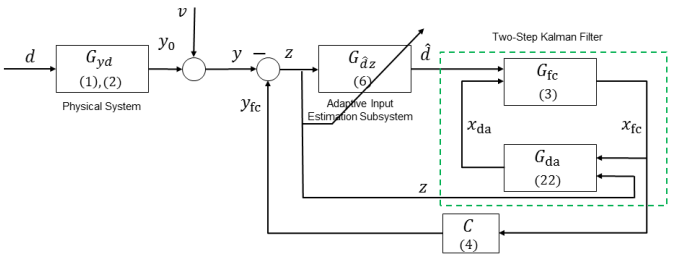

Fig. 1. Block diagram of RCIE. The two-step Kalman filter consists of the forecast subsystem G_{fc} and the data-assimilation subsystem G_{da}. The innovation z and the output $\hat{d}$ of the input-estimation subsystem $G_{\hat{d}z}$ are the inputs of the two-step Kalman filter.

Furthermore, (10) and (29) imply

$$z_{rc}(\hat{\theta},k) = C(k)\left(\prod_{i=1}^{n}\bar{A}(k-i)\right)x_{fc}(k-n) + \sum_{i=1}^{n}H_i(k)d_{rc}(\hat{\theta},k-i) + \sum_{i=1}^{n}H_i'(k)y(k-i) - y(k). \tag{32}$$

Subtracting (29) from (32) yields

$$z_{rc}(\hat{\theta},k) = z(k) + \sum_{i=1}^{n}H_i(k)\frac{1}{\mathbf{q}^i}[d_{rc}(\hat{\theta},k) - \hat{d}(k)]. \tag{33}$$

Hence, $G_{f,k}(\mathbf{q})$ in (11) is the FIR filter

$$G_{f,k}(\mathbf{q}) = \sum_{i=1}^{n_f}H_i(k)\frac{1}{\mathbf{q}^i} \tag{34}$$

and, thus, for all $k \geq 0$ and all $i = 1,\ldots,n_f$, $A_i(k) = 0$ and $K_i(k) = H_i(k)$ in (9) and (8), respectively. Furthermore, Φ_f and $\hat{d}_f$ defined by (12) and (13) are given by

$$\Phi_f(k) = \sum_{i=1}^{n_f}H_i(k)\Phi(k-i) \tag{35}$$

$$\hat{d}_f(k) = \sum_{i=1}^{n_f}H_i(k)\hat{d}(k-i). \tag{36}$$

D. Transfer Function Representation of RCIE

The physical system $G_{yd,k}$, forecast subsystem $G_{fc,k}$, input-estimation subsystem $G_{\hat{d}z,k}$, and data-assimilation subsystem $G_{da,k}$ in Fig. 1 represent [(1) and (2)], (3), (6), and (22), respectively. For simplicity of presentation, the known input u and the process noise w are not shown in Fig. 1 and are omitted for the remainder of this section.

By substituting (26) into (4), y_{fc} is given by

$$y_{fc}(k) = G_{y_{fc}y,k}(\mathbf{q})y(k) + G_{y_{fc}\hat{d},k}(\mathbf{q})\hat{d}(k) \tag{37}$$

where

$$G_{y_{fc}y,k}(\mathbf{q}) = C(k)[\mathbf{q}I - \bar{A}(k)]^{-1}\bar{B}(k) \tag{38}$$

$$G_{y_{fc}\hat{d},k}(\mathbf{q}) = C(k)[\mathbf{q}I - \bar{A}(k)]^{-1}G(k). \tag{39}$$

Algorithm 1 Input and State Estimation

Choose $n_c \geq 1$, $n_f \geq 1$, $0 < \lambda \leq 1$, R_z, R_d, R_θ, and $V_{\hat{d}}$.
$k_n = max(n_c, n_f)$;
Initialize: $\hat{d}(0) = 0$; $x_{da}(0) = \mathbf{E}[x(0)]$; $P_{da}(0) = \mathbf{E}[(x(0) - x_{da}(0))^T(x(0) - x_{da}(0))]$; $\theta(k_n) = 0_{l_\theta}$; $P(k_n-1) = R_\theta^{-1}$;
for $k = 1$ **to** N **do**
▷ Forecast Step
$x_{fc}(k) = A(k-1)x_{da}(k-1) + B(k-1)u(k-1) + G(k-1)\hat{d}(k-1)$;
$z(k) = C(k)x_{fc}(k) - y(k)$;
▷ Input Estimation
if $k \geq k_n$ **do**
$\Phi(k) = \left[\hat{d}(k-1)^T \cdots \hat{d}(k-n_c)^T\, z(k)^T \cdots z(k-n_c)^T\right] \otimes I_{l_d}$;
$\bar{A}(k-1) = A(k-1)[I_{l_x} + K_{da}(k-1)C(k-1)]$;
$\tilde{H}(k) = \left[C(k)G(k-1)\ H_2(k) \cdots H_{n_f}(k)\right]$, where $H_i(k) = C(k)\left(\prod_{j=1}^{i-1}\bar{A}(k-j)\right)G(k-i)$;
$\Phi_f(k) = \tilde{H}(k)\left[\Phi(k-1)^T \cdots \Phi(k-n_f)^T\right]^T$;
$\hat{d}_f(k) = \tilde{H}(k)\left[\hat{d}(k-1)^T \cdots \hat{d}(k-n_f)^T\right]^T$;
$\tilde{\Phi}(k) = \left[\Phi_f(k)^T\ \Phi(k)^T\right]^T$;
$\tilde{R}(k) = blockdiag(R_z, R_d)$;
$\tilde{z}(k) = \left[[z(k) - \hat{d}_f(k)]^T\ 0_{1\times l_d}\right]^T$;
$\Gamma(k) = [\lambda\tilde{R}(k)^{-1} + \tilde{\Phi}(k)P(k-1)\tilde{\Phi}(k)^T]^{-1}$;
$P(k) = \lambda^{-1}[P(k-1) - P(k-1)\tilde{\Phi}(k)^T\Gamma(k)\tilde{\Phi}(k)P(k-1)]$;
$\theta(k) = \theta(k-1) - P(k-1)\tilde{\Phi}(k)^T\Gamma(k)[\tilde{\Phi}(k)\theta(k-1) + \tilde{z}(k)]$;
$\hat{d}(k) = \Phi(k)\theta(k)$; ▷ Input estimate.
else do
$\hat{d}(k) = \hat{d}(0)$;
end if
▷ Data-Assimilation Step
$P_f(k) = A(k-1)P_{da}(k-1)A(k-1)^T + V_1(k-1) + V_{\hat{d}}(k-1)$;
$K_{da}(k) = -P_f(k)C(k)^T[C(k)P_f(k)C(k)^T + V_2(k)]^{-1}$;
$P_{da}(k) = [I_{l_x} + K_{da}(k)C(k)]P_f(k)$;
$x_{da}(k) = x_{fc}(k) + K_{da}(k)z(k)$; ▷ State estimate.
end for

Next, it follows from (6) that $\hat{d}$ is given by:

$$\hat{d}(k) = G_{\hat{d}z,k}(\mathbf{q})z(k) \tag{40}$$

where

$$G_{\hat{d}z,k}(\mathbf{q}) = (I_{l_d} - P_1(k)\mathbf{q}^{-1} - \cdots - P_{n_c}(k)\mathbf{q}^{-n_c})^{-1} \cdot (Q_0(k) + Q_1(k)\mathbf{q}^{-1} + \cdots + Q_{n_c}\mathbf{q}^{-n_c}). \tag{41}$$

Next, it follows from (1) and (2) that y is given by:

$$y(k) = G_{yd,k}(\mathbf{q})d(k) + D_2(k)v(k) \tag{42}$$

where

$$G_{yd,k}(\mathbf{q}) = C(k)[\mathbf{q}I - A(k)]^{-1}G(k). \tag{43}$$

Using (37), (40), and (42), the innovation z defined by (5) is given by

$$z(k) = G_{zd,k}(\mathbf{q})d(k) + G_{zy,k}(\mathbf{q})D_2(k)v(k) \tag{44}$$

where

$$G_{zy,k} = [I_{l_y} - G_{y_{fc}\hat{d},k}G_{\hat{d}z,k}]^{-1}[G_{y_{fc}y,k} - I_{l_y}] \quad (45)$$

$$G_{zd,k} = G_{zy,k}G_{yd,k}. \quad (46)$$

Using (40) and (44), $\hat{d}$ is given by

$$\hat{d}(k) = G_{\hat{d}d,k}(\mathbf{q})d(k) + G_{\hat{d}v,k}(\mathbf{q})v(k) \quad (47)$$

where

$$G_{\hat{d}d,k} = G_{\hat{d}z,k}G_{zd,k} \quad (48)$$

$$G_{\hat{d}v,k} = G_{\hat{d}z,k}G_{zy,k}D_2(k). \quad (49)$$

Now, define the notation

$$G_{yd,k} \triangleq D^{-1}_{yd,k}N_{yd,k} \in \mathbb{R}^{l_y\times l_d}(\mathbf{q}) \quad (50)$$

$$G_{y_{fc}y,k} \triangleq D^{-1}_{y_{fc}y,k}N_{y_{fc}y,k} \in \mathbb{R}^{l_y\times l_y}(\mathbf{q}) \quad (51)$$

$$G_{y_{fc}\hat{d},k} \triangleq D^{-1}_{y_{fc}\hat{d},k}N_{y_{fc}\hat{d},k} \in \mathbb{R}^{l_y\times l_d}(\mathbf{q}) \quad (52)$$

$$G_{\hat{d}z,k} \triangleq D^{-1}_{\hat{d}z,k}N_{\hat{d}z,k} \in \mathbb{R}^{l_d\times l_y}(\mathbf{q}) \quad (53)$$

and note from (38) and (39) that $D_{y_{fc}\hat{d},k} = D_{y_{fc}y,k}$. Using (51) and (53), it follows that (46) and (48) are given by:

$$G_{zd,k} = \big(I_{l_y} - D^{-1}_{y_{fc}\hat{d},k}N_{y_{fc}\hat{d},k}D^{-1}_{\hat{d}z,k}N_{\hat{d}z,k}\big)^{-1} \cdot \big(D^{-1}_{y_{fc}y,k}N_{y_{fc}y,k} - I_{l_y}\big)D^{-1}_{yd,k}N_{yd,k} \quad (54)$$

$$G_{\hat{d}d,k} = D^{-1}_{\hat{d}z,k}N_{\hat{d}z,k}\big(I_{l_y} - D^{-1}_{y_{fc}\hat{d},k}N_{y_{fc}\hat{d},k}D^{-1}_{\hat{d}z,k}N_{\hat{d}z,k}\big)^{-1} \cdot \big(D^{-1}_{y_{fc}y,k}N_{y_{fc}y,k} - I_{l_y}\big)D^{-1}_{yd,k}N_{yd,k}. \quad (55)$$

III. Analysis of the Input Estimation Subsystem

We now analyze the input-estimation subsystem $G_{\hat{d}z,k}$ in order to determine conditions on $G_{\hat{d}z,k}$ under which $z(k)$ and $\hat{d}(k)-d(k)$ converge to zero. We then show that RCIE adapts $G_{\hat{d}z,k}$ so as to satisfy these conditions.

In the following analysis, we assume for simplicity that A, C, G, K_{da}, and $G_{\hat{d}z}$ are time invariant. Furthermore, as a special case, assume that $l_d = l_y = 1$ and $u = w = v = 0$. Then, using (54) and (55), it follows that (44) and (47) are given by:

$$z(k) = G_{zd}(\mathbf{q})\,d(k) = \frac{N_{yd}(\mathbf{q})(N_{y_{fc}y}(\mathbf{q})-D_{y_{fc}y}(\mathbf{q}))D_{y_{fc}\hat{d}}(\mathbf{q})D_{\hat{d}z}(\mathbf{q})}{D_{yd}(\mathbf{q})D_{y_{fc}y}(\mathbf{q})\big(D_{y_{fc}\hat{d}}(\mathbf{q})D_{\hat{d}z}(\mathbf{q})-N_{y_{fc}\hat{d}}(\mathbf{q})N_{\hat{d}z}(\mathbf{q})\big)}d(k) \quad (56)$$

$$\hat{d}(k) = G_{\hat{d}d}(\mathbf{q})\,d(k) = \frac{N_{\hat{d}z}(\mathbf{q})N_{yd}(\mathbf{q})(N_{y_{fc}y}(\mathbf{q})-D_{y_{fc}y}(\mathbf{q}))D_{y_{fc}\hat{d}}(\mathbf{q})}{D_{yd}(\mathbf{q})D_{y_{fc}y}(\mathbf{q})\big(D_{y_{fc}\hat{d}}(\mathbf{q})D_{\hat{d}z}(\mathbf{q})-N_{y_{fc}\hat{d}}(\mathbf{q})N_{\hat{d}z}(\mathbf{q})\big)}d(k). \quad (57)$$

In the following analysis, we replace the forward shift operator $\mathbf{q}$ with the $\mathcal{Z}$-transform variable "z" in order to use the final value theorem. The identity

$$\det(zI - A - BC) = \det(zI - A) - C\mathrm{adj}(zI - A - BKC)B \quad (58)$$

implies that

$$\begin{aligned} D_{y_{fc}y}(z) - N_{y_{fc}y}(z) &= \det(zI - \bar{A}) - C\mathrm{adj}(zI - \bar{A})\bar{B} \\ &= \det(zI - A - AK_{da}C) + C\mathrm{adj}(zI - A - AK_{da}C)AK_{da} \\ &= \det(zI - A) - C\mathrm{adj}(zI - A - AK_{da}C)AK_{da} \\ &\quad + C\mathrm{adj}(zI - A - AK_{da}C)AK_{da} \\ &= \det(zI - A) = D_{yd}(z). \end{aligned} \quad (59)$$

Since $\bar{A} = A + AK_{da}C$, it follows from (38) and (43) that $N_{y_{fc}\hat{d}} = N_{yd}$. Using (59), $D_{y_{fc}\hat{d}} = D_{y_{fc}y}$, and $N_{y_{fc}\hat{d}} = N_{yd}$, it follows from (56) and (57) that:

$$\mathcal{Z}\{z\}(z) = G_{zd}(z)\,\mathcal{Z}\{d\}(z) = \frac{N_{yd}(z)D_{\hat{d}z}(z)}{N_{y_{fc}\hat{d}}(z)N_{\hat{d}z}(z) - D_{y_{fc}\hat{d}}(z)D_{\hat{d}z}(z)}\mathcal{Z}\{d\}(z) \quad (60)$$

$$\mathcal{Z}\{\hat{d}\}(z) = G_{\hat{d}d}(z)\,\mathcal{Z}\{d\}(z) = \frac{N_{\hat{d}z}(z)N_{yd}(z)}{N_{y_{fc}\hat{d}}(z)N_{\hat{d}z}(z) - D_{y_{fc}\hat{d}}(z)D_{\hat{d}z}(z)}\mathcal{Z}\{d\}(z). \quad (61)$$

As an example, assume that $d(k) \equiv \bar{d}$ is constant and $G_{\hat{d}z}$ has an internal model of d, that is, $D_{\hat{d}z}(z) = (z-1)\bar{D}_{\hat{d}z}(z)$. Then,

$$\mathcal{Z}\{d\}(z) = \frac{\bar{d}}{z-1}, \quad G_{\hat{d}z}(z) = \frac{N_{\hat{d}z}(z)}{(z-1)\bar{D}_{\hat{d}z}(z)}. \quad (62)$$

Using (60) and assuming that $N_{y_{fc}\hat{d}}(z)N_{\hat{d}z}(z) - (z-1)D_{y_{fc}\hat{d}}(z)\bar{D}_{\hat{d}z}(z)$ is asymptotically stable, it follows from the final value theorem that:

$$\lim_{k\to\infty} z(k) = \lim_{z\to 1}(z-1)\frac{(z-1)N_{yd}(z)\bar{D}_{\hat{d}z}(z)}{N_{y_{fc}\hat{d}}(z)N_{\hat{d}z}(z)-(z-1)D_{y_{fc}\hat{d}}(z)\bar{D}_{\hat{d}z}(z)}\cdot\frac{\bar{d}}{(z-1)} = 0. \quad (63)$$

Similarly, using (61) and $N_{y_{fc}\hat{d}} = N_{yd}$, it follows that:

$$\lim_{k\to\infty}\hat{d}(k) = \left.\frac{N_{\hat{d}z}(z)N_{yd}(z)}{N_{y_{fc}\hat{d}}(z)N_{\hat{d}z}(z) - (z-1)D_{y_{fc}\hat{d}}(z)\bar{D}_{\hat{d}z}(z)}\right|_{z=1}\bar{d} = \bar{d}. \quad (64)$$

To apply the above analysis, we assume that the unknown input $d(k)$ is generated by the discrete-time, linear time-invariant exogenous subsystem

$$x_d(k) = A_d x_d(k-1) \quad (65)$$

$$d(k) = C_d x_d(k) \quad (66)$$

where $A_d \in \mathbb{R}^{n\times n}$, $C_d \in \mathbb{R}^{l_d\times n}$, and the eigenvalues of A_d are simple and lie on the unit circle. Now, assume that the following conditions are satisfied.

P1: $G_{\hat{d}z}$ contains an internal model of d, that is, for all $\lambda \in \mathrm{spec}(A_d)$, $|G_{\hat{d}z}(\lambda)| = \infty$.

P2: $N_{y_{fc}\hat{d}}N_{\hat{d}z} - D_{y_{fc}\hat{d}}D_{\hat{d}z}$ is asymptotically stable.
P3: For all $\lambda \in \text{spec}(A_d)$, $G_{\hat{d}d}(\lambda) = 1$.

Then, it follows from the internal model principle [52] that, as $k \to \infty$, $z(k) \to 0$ and $\hat{d}(k) - d(k) \to 0$. The following examples show that RCIE adapts $G_{\hat{d}z,k}$ such that P1–P3 are asymptotically satisfied.

Example 1: Consider the MP system

$$G_{yd}(z) = \frac{z - 0.9}{(z - 0.7)(z - 0.8)} \tag{67}$$

with the minimal realization

$$A = \begin{bmatrix} 1.5 & -0.56 \\ 1 & 0 \end{bmatrix}, \quad G = \begin{bmatrix} 1 \\ 0 \end{bmatrix}, \quad C = [1 \ \ -0.9]. \tag{68}$$

Let $n_c = 3, n_f = 24, \lambda = 1, R_\theta = 10^{-4}I_{l_\theta}$, $R_d = 10^{-6}$, $R_z = 1$, and $V_{\hat{d}} = 10^{-2}I_{l_x}$, and let B, V_1, and V_2 be zero. The unknown input is $d(k)$=1+ sin(0.3k), which consists of a step and a harmonic. Its $\mathcal{Z}$-transform is given by

$$\mathcal{Z}\{d\}(z) = \frac{z}{z - 1} + 0.29\frac{z}{z^2 - 1.91z + 1}. \tag{69}$$

Note that, since the input d is unknown, the frequency of its harmonic component is unknown to RCIE. It, thus, is not possible to construct an auxiliary system that captures the spectrum of d.

After an initial transient of 10 time steps, $\hat{d}$ follows d, as shown in Fig. 2(a). The estimator coefficients $\theta(k)$ shown in Fig. 2(b) converge in 50 steps to

$$G_{\hat{d}z,50}(z) = -2.91\frac{(z + 0.006)(z^2 - 0.99z + 0.34)}{(z - 1.004)(z^2 - 1.909z + 0.999)}. \tag{70}$$

The poles of $G_{\hat{d}z,50}$ at 1.004 and $0.95 \pm 0.29\jmath$ in (70) show that RCIE builds an internal model of d in $G_{\hat{d}z,50}$. Thus, P1 is satisfied. Furthermore, K_{da} (not shown in Fig. 2) also converges, and the poles of $G_{\hat{d}d,50}$ are shown in Fig. 2(c). Since the poles of $G_{\hat{d}d,50}$ are inside the open unit disk, P2 is satisfied. The magnitude and phase plots of $G_{\hat{d}d,50}$ in Fig. 2(d) show that, at both dc and the unknown input frequency 0.3 rad/s, the magnitude is 1 and the phase is 0°. Hence, P3 is satisfied.

To test the robustness of RCIE to model error, we vary the (1, 2) entry of A matrix while keeping G, C constant. The RCIE parameters are kept the same for all cases. Fig. 3 shows the mean and standard deviation of the error $|d - \hat{d}|$, after 50 time steps, for a range of values of the (1, 2) entry of A. Note that the mean and standard deviation of the error increase linearly as the (1, 2) entry of A varies from its true value 0.56. ◊

Example 2: Consider the NMP system

$$G_{yd}(z) = \frac{z - 1.2}{(z - 0.7)(z - 0.8)} \tag{71}$$

with the minimal realization

$$A = \begin{bmatrix} 1.5 & -0.56 \\ 1 & 0 \end{bmatrix}, \quad G = \begin{bmatrix} 2 \\ 0 \end{bmatrix}, \quad C = [0.5 \ \ -0.6]. \tag{72}$$

The tuning parameters are the same as in Example 1. The unknown input is $d(k)$= sin(0.3k).

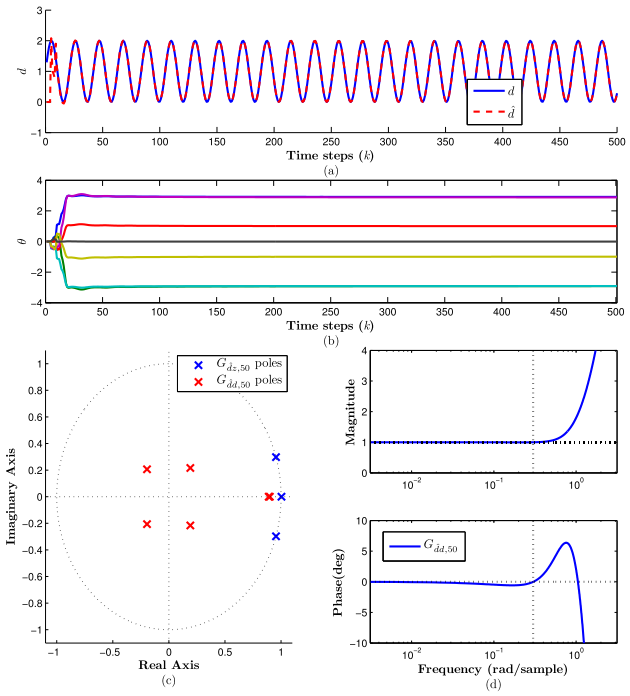

Fig. 2. RCIE for the MP system (67). (a) After the initial transient, $\hat{d}$ follows d. (b) Estimator coefficients θ converge in about 50 steps. (c) Poles of $G_{\hat{d}z,50}$ at 1.004 and $0.95 \pm 0.29\jmath$ show that RCIE builds an internal model of d in $G_{\hat{d}z,50}$. The poles of $G_{\hat{d}d,50}$ are inside the open unit disk. (d) $G_{\hat{d}d,50}$ has magnitude 1 and phase 0° at both dc and the unknown input frequency 0.3 rad/s.

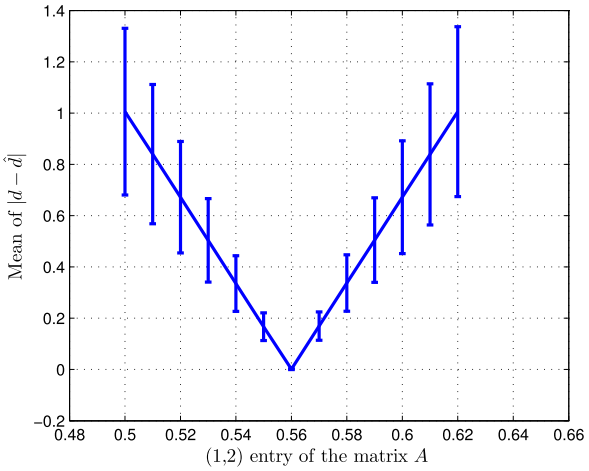

Fig. 3. Robustness of RCIE to model error for the system (67). The (1, 2) entry of A is varied while keeping the matrices G, C, and RCIE parameters constant. Note that the mean and standard deviation of the error increase linearly as the (1, 2) entry of A varies from its true value 0.56.

After an initial transient of about 90 steps, $\hat{d}$ follows d, as shown in Fig. 4(a). The estimator coefficients $\theta(k)$ shown in Fig. 4(b) converge in about 450 steps to

$$G_{\hat{d}z,450}(z) = 8.52\frac{(z + 0.01)(z^2 - 1.908z + 0.91)}{(z + 10.46)(z^2 - 1.903z + 0.99)}. \tag{73}$$

The poles of $G_{\hat{d}z,450}$ at $0.95 \pm 0.29\jmath$ in (73) show that RCIE builds an internal model of d in $G_{\hat{d}z,450}$. Thus, P1 is satisfied. Furthermore, K_{da} (not shown in Fig. 2) also converges, and

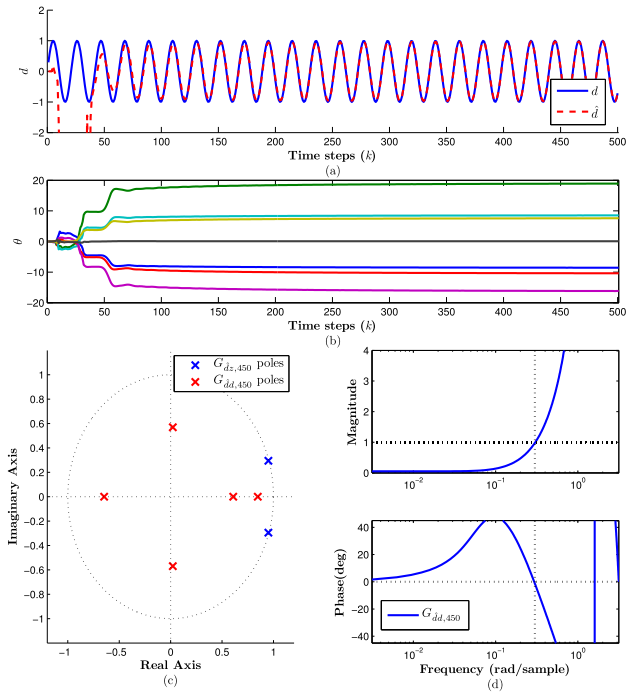

Fig. 4. RCIE for the NMP system (71). (a) After the initial transient, $\hat{d}$ follows d. (b) Estimator coefficients θ converge in about 450 steps. (c) Poles of $G_{\hat{d}z,450}$ at $0.95 \pm 0.29\jmath$ show that RCIE builds an internal model of d in $G_{\hat{d}z}$. The poles of $G_{\hat{d}d,450}$ are inside the open unit disk. (d) $G_{\hat{d}d}$ has magnitude 1 and phase 0° at the unknown input frequency 0.3 rad/s.

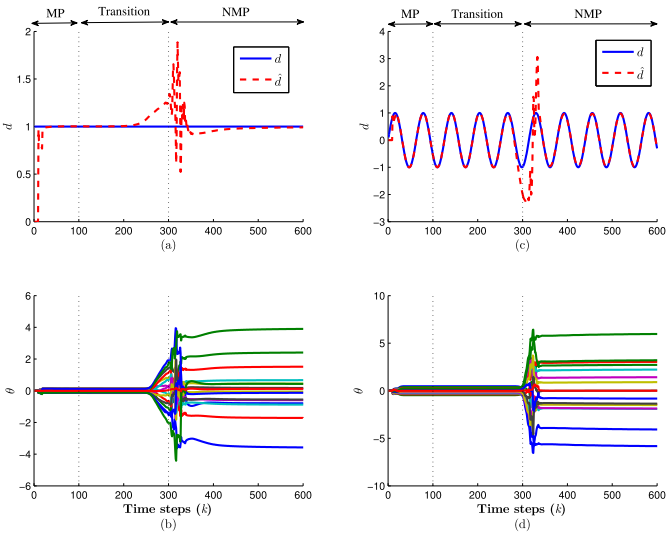

Fig. 5. RCIE for the time-varying system (74). The transition begins at $k = 100$ steps and ends at $k = 300$ steps. (a) RCIE estimates constant d for both MP and NMP G_{yd} with an intervening transient response. (b) Estimator coefficients readapt due to the transition of G_{yd} from MP to NMP dynamics in order to estimate d. (c) RCIE estimates harmonic d for both MP and NMP G_{yd} with an intervening transient response. (d) Estimator coefficients readapt due to the transition of G_{yd} from MP to NMP dynamics in order to estimate d.

the poles of $G_{\hat{d}d,450}$ are shown in Fig. 4(c). Since the poles of $G_{\hat{d}d,450}$ are inside the open unit disk, P2 is satisfied. The magnitude and phase plots of $G_{\hat{d}d,450}$ in Fig. 4(d) show that, at the unknown input frequency 0.3 rad/s, the magnitude is 1 and the phase is 0°. Hence, P3 is satisfied. $\diamondsuit$

Example 3: Consider the linear, time-varying system

$$G_{yd,k}(\mathbf{q}) = \frac{\mathbf{q} - \xi(k)}{(\mathbf{q} - 0.8)(\mathbf{q} - 0.9)} \tag{74}$$

where

$$\xi(k) = \begin{cases} 0.95, & k < 100 \\ 0.95 + 0.001(k - 100), & 100 \le k \le 300 \\ 1.15, & k > 300. \end{cases} \tag{75}$$

Note that, during the transition, G_{yd} is MP for $k < 150$ and NMP for $k \ge 150$. Let $n_c = 8$, $n_f = 48$, $\lambda = 0.998$, $R_\theta = 10^{-2} I_{l_\theta}$, $R_d = 10^{-6}$, $R_z = 1$, and $V_{\hat{d}} = 10^{-2} I_{l_x}$.

First, we consider the case where the unknown input $d(k)$ is constant. Fig. 5(a) shows that RCIE estimates d for both MP and NMP G_{yd} with an intervening transient. Fig. 5(b) shows that the estimator coefficients $\theta(k)$ readapt due to the transition of G_{yd} from MP to NMP dynamics in order to estimate d. Note that, at $k = 100$ and 600 steps, $G_{\hat{d}z,k}$ has a pole at 1, $G_{\hat{d}d,k}$ is asymptotically stable, and $G_{\hat{d}d,k}(1) \approx 1$. Hence, before and after the transition, P1–P3 are satisfied.

Next, we consider the case where $d(k) = \sin(0.1k)$. Fig. 5(c) shows that RCIE estimates d for both MP and NMP G_{yd} with an intervening transient. Fig. 5(d) shows that the estimator coefficients $\theta(k)$ readapt due to the transition of G_{yd} from MP to NMP dynamics in order to estimate d. Note that, at $k = 100$ and 600 steps, $G_{\hat{d}z,k}$ has poles at 0.995 ± 0.099, $G_{\hat{d}d,k}$ is asymptotically stable, and $G_{\hat{d}d}(e^{0.1\jmath}) \approx 1$. Hence, before and after the transition, P1–P3 are satisfied. $\diamondsuit$

IV. Effect of the Unobservable Input Subspace

As shown in [24], if (A, G, C) has an invariant zero, then it has a nontrivial unobservable input subspace. In particular, an input of the form $d(k) = \mathrm{Re}(\xi^k \bar{d})$, where $\xi \in \mathbb{C}$ is an invariant zero of (A, G, C) and $\bar{d} \in \mathbb{C}^{l_d}$ is specified in Example 4 in the following, is unobservable, since there exists an initial condition $x(0) = \mathrm{Re}(\bar{x})$ such that the output is identically zero. Note that, for each example in Section III, the input d was chosen so that its spectral content is disjoint from the zeros of (A, G, C). For instance, in Example 1, d is the sum of step and harmonic signals, but the zero of G_{yd} is 0.9. This section illustrates the effect of the unobservable input subspace in the case where the unknown input has spectral content that coincides with a zero of (A, G, C).

Example 4: Consider the system

$$G_{yd}(z) = C(zI - A)^{-1}G = \frac{z - \xi}{(z - 0.7)(z - 0.8)} \tag{76}$$

where $\xi \in \mathbb{C}$ is an invariant zero of (A, G, C). Let

$$\begin{bmatrix} \bar{x} \\ \bar{d} \end{bmatrix} \in \mathcal{N}\left(\begin{bmatrix} \xi I - A & -G \\ C & 0 \end{bmatrix} \right)$$

be nonzero with nonzero real part and define $d(k) = d_{ob}(k) + d_{uo}(k)$, where, for all $k \ge 0$, $d_{ob}(k) = \sin(0.3k)$ and $d_{uo}(k) = \mathrm{Re}(\xi^k \bar{d})$. Furthermore, let $x(0) = \mathrm{Re}(\bar{x})$. Note that d_{uo} is unobservable. Next, let $n_c = 8$, $n_f = 48$, $\lambda = 0.998$, $R_\theta = 10^{-2} I_{l_\theta}$, $R_d = 10^{-6}$, $R_z = 1$, and $V_{\hat{d}} = 10^{-2} I_{l_x}$.

First, let $\xi = 0.96$, which lies in the open unit disk. In this case, Fig. 6(a) shows that $\hat{d}$ converges to d_{ob}. Furthermore,

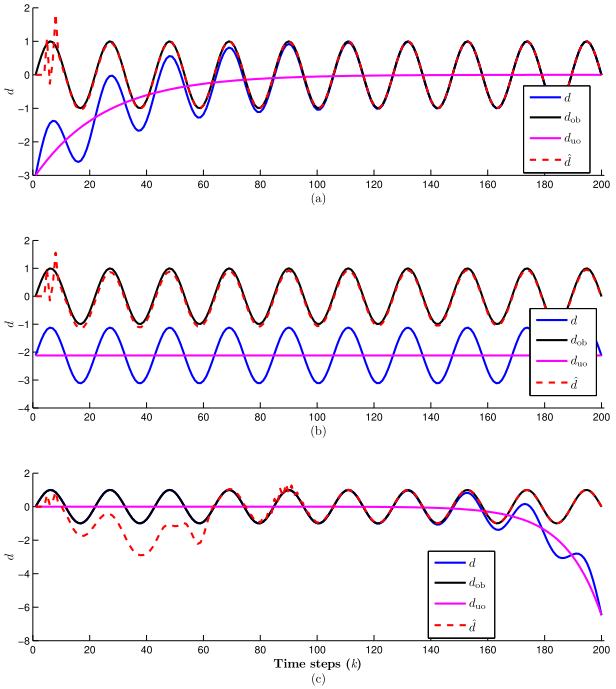

Fig. 6. Effect of the unobservable input subspace on the estimate of the unknown input using RCIE for the system (76). (a) $\hat{d}$ converges to d_{ob}, and $d_{uo} = d - d_{ob}$ converges to zero. (b) $\hat{d}$ converges to d_{ob}, and $d_{uo} = d - d_{ob}$ is a nonzero constant. (c) $\hat{d}$ converges to d_{ob}, and $d_{uo} = d - d_{ob}$ diverges.

Fig. 6(a) shows that $d - d_{ob}$ converges to zero, which is consistent with the fact that $d_{uo} = d - d_{ob}$ converges to zero. Thus, $d - \hat{d}$ also converges to zero.

Next, let $\xi = 1$, which lies on the unit circle. In this case, Fig. 6(b) shows that $\hat{d}$ converges to d_{ob}. Furthermore, Fig. 6(b) shows that $d - d_{ob}$ does not converge to zero, which is consistent with the fact that d_{uo} is constant. Thus, $d - \hat{d}$ converges to d_{uo}.

Finally, let $\xi = 1.08$, which lies outside the closed unit disk. In this case, Fig. 6(c) shows that $\hat{d}$ converges to d_{ob}. Furthermore, Fig. 6(c) shows that $d - d_{ob}$ diverges, which is consistent with the fact that d_{uo} diverges. Thus, $d - \hat{d}$ also diverges; however, $d_{ob} - \hat{d}$ converges to zero.

Note that, in all three cases, $\hat{d}$ converges to d_{ob} and z (not shown in Fig. 6) converges to zero after an initial transient. $\Diamond$

V. Comparison of RCIE With ULISE

We now compare RCIE with the ULISE filter [30] in the presence of process and measurement noise. To assess the accuracy of the input estimate, we plot the error metrics

$$e_{\mathrm{RCIE}}(k) \triangleq \frac{1}{N_{\mathrm{trial}}} \sqrt{\sum_{i=1}^{N_{\mathrm{trial}}} [\hat{d}_i(k) - d(k)]^2} \tag{77}$$

$$e_{\mathrm{ULISE}}(k) \triangleq \frac{1}{N_{\mathrm{trial}}} \sqrt{\sum_{i=1}^{N_{\mathrm{trial}}} [\hat{d}_{\mathrm{ULISE,i}}(k) - d(k)]^2} \tag{78}$$

where i denotes the ith trial, $\hat{d}_i$ is the ith RCIE estimate of d, $\hat{d}_{\mathrm{ULISE,i}}$ is the ith ULISE estimate of d, and N_{trial} is the number of trials. Each trial is based on a randomly generated realization of v and w.

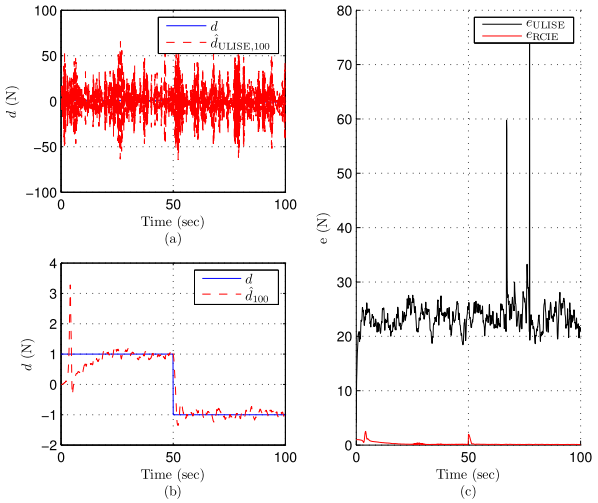

Fig. 7. Estimation of a multistep input for the lightly damped mass-spring-damper system (79). (a) UILSE estimate. (b) RCIE estimate. (c) Error in the input estimate. The error for RCIE has mean 0.2 N and standard deviation 0.3 N, whereas the error for ULISE has mean 23.5 N and standard deviation 3.3 N.

Example 5: Consider the mass-spring-damper system with masses m_1 and m_2 and input force d applied to m_1. The dynamics are given by

$$\dot{x} = A_c x + G_c d \tag{79}$$

where

$$A_c \triangleq \begin{bmatrix} 0_{2\times 2} & I_{2\times 2} \\ \Omega_1 & \Omega_2 \end{bmatrix}, \quad G_c \triangleq \begin{bmatrix} 0_{2\times 1} \\ \Omega_3 \end{bmatrix}$$

$$\Omega_1 \triangleq \begin{bmatrix} -\frac{k_1+k_2}{m_1} & \frac{k_2}{m_1} \\ \frac{k_2}{m_2} & -\frac{k_2}{m_2} \end{bmatrix}, \quad \Omega_2 \triangleq \begin{bmatrix} -\frac{c_1+c_2}{m_1} & \frac{c_2}{m_1} \\ \frac{c_2}{m_2} & -\frac{c_2}{m_2} \end{bmatrix}$$

$$\Omega_3 \triangleq \begin{bmatrix} \frac{1}{m_1} \\ 0 \end{bmatrix}$$

x_1 and x_2 are the displacements and x_3 and x_4 are the velocities of masses m_1 and m_2, respectively. We choose $m_1 = m_2 = 1\,\mathrm{kg}$, $k_1 = k_2 = 1\,\mathrm{N/m}$, and $c_1 = c_2 = 1\,\mathrm{kg/s}$. We discretize (79) as

$$A = e^{A_c T_s}, \quad G = A_c^{-1}(A_c - I)G_c \tag{80}$$

where $T_s = 0.1\,\mathrm{s}$ is the sampling time. The discretized system has poles at $0.87 \pm 0.08\jmath$ and $0.97 \pm 0.05\jmath$. Letting

$$C = \begin{bmatrix} 1 & 0 & 0 & 0 \\ 0 & 1 & 0 & 0 \end{bmatrix}$$

we measure the positions and estimate the velocities and the unknown input force d on m_1. The system (A, G, C) has no invariant zeros. Let $N_{\mathrm{trial}} = 100$, $n_c = 4$, $n_f = 24$, $\lambda = 1$, $R_\theta = 10^{-2} I_{l_\theta}$, $R_d = 10^{-8}$, $R_z = I_{l_y}$, $V_{\hat{d}} = 0$, $D_1 = 10^{-2}\mathrm{diag}(1, 1, 2, 2)$, and $D_2 = 10^{-2}\mathrm{diag}(1, 1)$.

First, we consider the case where the unknown input force d is a multistep. Fig. 7 shows that the error for RCIE has

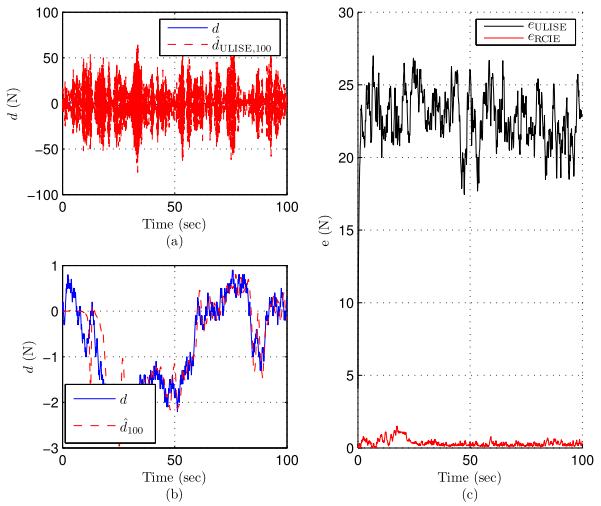

Fig. 8. Estimation of an unknown random-walk input for the lightly damped, mass-spring-damper system (79). (a) ULISE estimate. (b) RCIE estimate. (c) Error in the input estimate. The RCIE error has mean 0.3 N and standard deviation 0.2 N, whereas the ULISE error has mean 22.6 N and standard deviation 2.1 N.

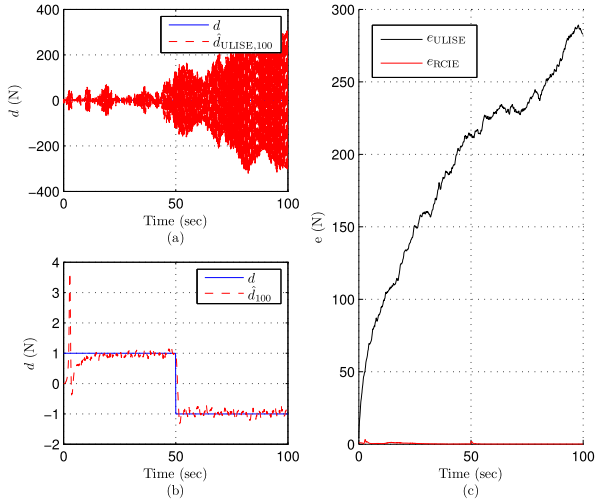

Fig. 9. Estimation of an unknown multistep input for the mass-spring system (79) with $c_1 = c_2 = 0$. (a) ULISE estimate. (b) RCIE estimate. (c) Error in the input estimate. The RCIE error is close to zero, whereas the ULISE error diverges.

mean 0.2 N and standard deviation 0.3 N, whereas the error for ULISE has mean 23.5 N and standard deviation 3.3 N. Next, we consider the case where the unknown input force is a random walk. At each time step k, the random walk is modeled as an increase or decrease in the magnitude by 0.1 N with equal probability. Fig. 8 shows that the RCIE error has mean 0.3 N and standard deviation 0.2 N, whereas the ULISE error has mean 22.6 N and standard deviation 2.1 N. ◊

Example 6: Reconsider the system (79) but with zero damping, that is, $c_1 = c_2 = 0$. Hence, (79) is Lyapunov stable but not asymptotically stable. The continuous-time system has no transmission zeros, but the discretized system (A, G, C) has one transmission zero at -1 due to the sampling.

We consider the case where the unknown input force d is a multistep. Fig. 9 shows that the RCIE error is 0.1 N at $t = 100$ s, whereas the ULISE error diverges and is 282.7 N at $t = 100$ s. The behavior of the error shown in Fig. 9(c) with ULISE for the NMP system is consistent with the fact that [30, Th. 6] is confined to MP systems. ◊

VI. Experimental Application: Estimation of Inertial Acceleration

A. Problem Description

The Earth frame and body-fixed frame are denoted by F_E and F_B, respectively. We assume that F_E is an inertial frame and the Earth is flat. The origin O_E of F_E is any convenient point fixed on the Earth. The axes $\hat{\imath}_E$ and $\hat{\jmath}_E$ are horizontal, while the axis $\hat{k}_E$ points downward. F_B is defined with $\hat{\imath}_B$, $\hat{\jmath}_B$, and $\hat{k}_B$ fixed relative to the body. F_B and F_E are related by

$$F_B = \vec{R}_{B/E}\, F_E \tag{81}$$

where $\vec{R}_{B/E}$ is a physical rotation matrix represented by a 3-2-1 Euler rotation sequence, involving two intermediate frames $F_{E'}$ and $F_{E''}$. In particular,

$$\vec{R}_{B/E} = \vec{R}_{\hat{\imath}_{E''}}(\Phi)\, \vec{R}_{\hat{\jmath}_{E'}}(\Theta)\, \vec{R}_{\hat{k}_E}(\Psi) \tag{82}$$

where $F_{E'} = \vec{R}_{E'/E}\, F_E$, $F_{E''} = \vec{R}_{E''/E'}\, F_{E'}$, and $\vec{R}_{\hat{n}}(\kappa)$ is the Rodrigues rotation about the eigenaxis $\hat{n}$ through the eigenangle κ according to the right-hand rule.

Let p denote a point that is fixed on the body. The location of p relative to O_E is denoted by $\vec{r}_{p/O_E}$ and is resolved in F_E as

$$\begin{bmatrix} X \\ Y \\ Z \end{bmatrix} \triangleq \vec{r}_{p/O_E}\big|_E. \tag{83}$$

The velocity of p relative to O_E with respect to F_E is given by

$$\vec{v}_{p/O_E/E} = \overset{E\bullet}{\vec{r}}_{p/O_E} \tag{84}$$

where $E\bullet$ denotes the derivative with respect to the time taken in Earth frame. The acceleration of p relative to O_E with respect to F_E is given by

$$\vec{a}_{p/O_E/E} = \overset{E\bullet}{\vec{v}}_{p/O_E/E} = \overset{E\bullet\bullet}{\vec{r}}_{p/O_E}. \tag{85}$$

We resolve $\vec{a}_{p/O_E/E}$ in F_E and F_B using the notation

$$\begin{bmatrix} A_x \\ A_y \\ A_z \end{bmatrix} \triangleq \vec{a}_{p/O_E/E}\big|_E, \quad \begin{bmatrix} a_x \\ a_y \\ a_z \end{bmatrix} \triangleq \vec{a}_{p/O_E/E}\big|_B. \tag{86}$$

Using (82) and (86), $\vec{a}_{p/O_E/E}$ in F_E is given by

$$\vec{a}_{p/O_E/E}\big|_E = \mathcal{O}_{E/B}\, \vec{a}_{p/O_E/E}\big|_B \tag{87}$$

and thus

$$\begin{bmatrix} A_x \\ A_y \\ A_z \end{bmatrix} = \mathcal{O}_{E/B} \begin{bmatrix} a_x \\ a_y \\ a_z \end{bmatrix} \tag{88}$$

where

$$\mathcal{O}_{E/B} = \vec{R}_{E/B}\,|_E.$$

Note that (81)–(88) are kinematic relations that are applicable to an arbitrary point p on a body and are independent of all modeling information.

For estimating the inertial acceleration of p relative to O_E with respect to F_E, (84)–(88) are written in state-space form

$$\dot{x} = A_c x + G_c d \tag{89}$$

where

$$A_c = \begin{bmatrix} 0_{3\times3} & I_{3\times3} \\ 0_{3\times3} & 0_{3\times3} \end{bmatrix}, \quad G_c = \begin{bmatrix} 0_{3\times3} \\ I_{3\times3} \end{bmatrix} \tag{90}$$

$$x = [X\ Y\ Z\ \dot{X}\ \dot{Y}\ \dot{Z}]^T, \quad d = [A_x\ A_y\ A_z]^T. \tag{91}$$

Note that (89) is an exact kinematic equation, and thus it does not include process noise. For estimating the inertial acceleration of p relative to O_E with respect to F_B, (84)–(88) are written in state-space form

$$\dot{x} = A_c x + G_c d + D_1 w \tag{92}$$

where

$$A_c = \begin{bmatrix} 0_{3\times3} & I_{3\times3} \\ 0_{3\times3} & 0_{3\times3} \end{bmatrix}, \quad G_c = \begin{bmatrix} 0_{3\times3} \\ \mathcal{O}_{E/B} \end{bmatrix} \tag{93}$$

$$x = [X\ Y\ Z\ \dot{X}\ \dot{Y}\ \dot{Z}]^T, \quad d = [a_x\ a_y\ a_z]^T. \tag{94}$$

Likewise, (92) is an exact kinematic equation; however, process noise is now included to account for errors in the measurements of the matrix $\mathcal{O}_{E/B}$ appearing in (93). Finally, note that, due to $\mathcal{O}_{E/B}$, (92) is a continuous-time linear, time-varying system; therefore, its discretization is linear, time-varying.

B. Experimental Setup

In the laboratory setup, we estimate the inertial acceleration of a quadrotor in F_E and F_B using (89) and (92), respectively, with $C = [I_{3\times3}\ 0_{3\times3}]$. The position $\vec{r}_{p/O_E}|_E$ and attitude (Φ, Θ, Ψ) of the vehicle are obtained using the Vicon system and recorded for postflight data analysis. To compare the estimated acceleration with the measured acceleration, data from the vehicle's inertial measurement unit (IMU) are recorded and time-stamped. Using knowledge of the vehicle attitude, IMU acceleration measurements are corrected to compensate for gravity offset for comparison with RCIE acceleration estimates.

C. Estimating Inertial Acceleration in the Earth Frame

We discretize (89) with $T_s = 0.01$ s, which is the sample rate of the recorded data. The system (A, G, C) is NMP with six poles at 1 and three invariant zeros at -1. Note that D_1 is zero. Let $n_c = 2$, $n_f = 6$, $\lambda = 1$, $R_\theta = 10^{-10} I_{l_\theta}$, $R_d = 10^{-2} I_{l_d}$, $R_z = I_{l_y}$, $V_{\hat{d}} = 10^{-4} I_{6\times6}$, and $V_2 = 10^{-2} I_{3\times3}$.

Fig. 10 shows the accuracy of the RCIE estimate of the inertial acceleration of the quadrotor in F_E using position measurements obtained from the Vicon system. For this setup, the estimates of d using filters [16] and [30] diverge in less than 2.5 s (not shown).

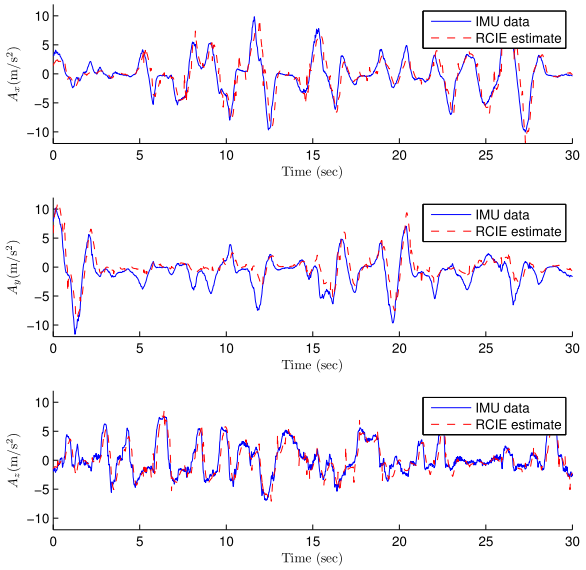

Fig. 10. Estimation of the inertial acceleration of the quadrotor relative to O_E with respect to F_E using position measurements. RCIE estimates are compared with the IMU acceleration measurements transformed to F_E and corrected to compensate for gravity offset.

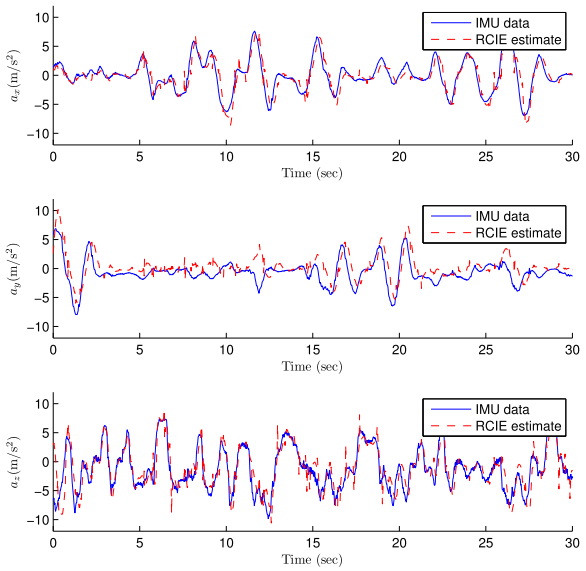

Fig. 11. Estimation of the inertial acceleration of the quadrotor relative to O_E with respect to F_B using position and attitude measurements. RCIE estimates are compared with the IMU acceleration measurements with gravity correction.

D. Estimating Inertial Acceleration in the Body Frame

Noting that G_c is time varying in (92), we discretize (92) at each time step k with $T_s = 0.01$ s, which is the sample rate of the recorded data. Let $n_c = 2$, $n_f = 6$, $\lambda = 1$, $R_\theta = 10^{-10} I_{l_\theta}$, $R_d = 10^{-4} I_{l_d}$, $R_z = I_{l_y}$, $V_{\hat{d}} + V_1 = 10^{-4} I_{6\times6}$, and $V_2 = 10^{-2} I_{3\times3}$.

Fig. 11 shows the accuracy of the RCIE estimate of the inertial acceleration of the quadrotor in the body frame using position and attitude measurements obtained from the Vicon system. For this setup, the estimates of d using filters [16] and [30] diverge in less than 2.5 s (not shown).

VII. Conclusion

This paper presented RCIE and showed that this algorithm is effective for asymptotically estimating the unknown input of an NMP system. The mechanism underlying RCIE was explained in terms of an internal model of the unknown input. In particular, RCIE was shown to automatically construct an internal model of the unknown input d despite the lack of knowledge of the spectrum of d and in the presence of arbitrary invariant zeros.

As an experimental application, RCIE was used to estimate the inertial acceleration of a UAV; these estimates were shown to be close to independent, onboard measurements provided by an IMU. In contrast, the techniques of [16] and [30] produced divergent estimates. In fact, the techniques in [16], [30], and [34] are not applicable to this problem due to the presence of invariant zeros on the unit circle.

Future research will focus on the following questions. First, the covariance $V_{\hat{d}}(k)$ of $\hat{d}(k)$ is required to update the forecast error covariance P_f given by (24). An online technique for setting this covariance is desirable. Next, alternative techniques for constructing G_f that are simpler than the method given in Section II-C could simplify the implementation of RCIE. Finally, stochastic analysis of RCIE in the case where the dynamics are linear time-varying remains a future objective.

Acknowledgment

The authors would like to thank D. Panagou and W. Ding for providing the camera and IMU data used in this paper. They would also like to thank a reviewer for bringing [36] and [37] to their attention.

References

[1] R. E. Kalman, "A new approach to linear filtering and prediction problems," *Trans. ASME D, J. Basic Eng.*, vol. 82, pp. 35–45, 1960.

[2] R. E. Kalman and R. S. Bucy, "New results in linear filtering and prediction theory," *J. Basic Eng.*, vol. 83, no. 1, pp. 95–108, 1961.

[3] D. Simon, *Optimal State Estimation: Kalman, H_∞, and Nonlinear Approaches*. Hoboken, NJ, USA: Wiley, 2006.

[4] F. L. Lewis, L. Xie, and D. Popa, *Optimal and Robust Estimation: With an Introduction to Stochastic Control Theory*. Boca Raton, FL, USA: CRC Press, 2007.

[5] J. L. Crassidis and J. L. Junkins, *Optimal Estimation of Dynamic Systems*. Boca Raton, FL, USA: CRC Press, 2011.

[6] B. Friedland, "Treatment of bias in recursive filtering," *IEEE Trans. Autom. Control*, vol. AC-14, no. 4, pp. 359–367, Aug. 1969.

[7] J. Glover, "The linear estimation of completely unknown signals," *IEEE Trans. Autom. Control*, vol. 14, no. 6, pp. 766–767, Jun. 1969.

[8] P. K. Kitanidis, "Unbiased minimum-variance linear state estimation," *Automatica*, vol. 23, no. 6, pp. 775–778, 1987.

[9] M. Darouach and M. Zasadzinski, "Unbiased minimum variance estimation for systems with unknown exogenous inputs," *Automatica*, vol. 33, no. 4, pp. 717–719, 1997.

[10] M. Hou and R. J. Patton, "Optimal filtering for systems with unknown inputs," *IEEE Trans. Autom. Control*, vol. AC-43, no. 3, pp. 445–449, Mar. 1998.

[11] M. Corless and J. Tu, "State and input estimation for a class of uncertain systems," *Automatica*, vol. 34, no. 6, pp. 757–764, 1998.

[12] C.-S. Hsieh and F.-C. Chen, "Optimal solution of the two-stage Kalman estimator," *IEEE Trans. Autom. Control*, vol. 44, no. 1, pp. 194–199, Jan. 1999.

[13] C.-S. Hsieh, "Robust two-stage Kalman filters for systems with unknown inputs," *IEEE Trans. Autom. Control*, vol. 45, no. 12, pp. 2374–2378, Dec. 2000.

[14] Y. Xiong and M. Saif, "Unknown disturbance inputs estimation based on a state functional observer design," *Automatica*, vol. 39, pp. 1389–1398, Aug. 2003.

[15] T. Floquet and J.-P. Barbot, "State and unknown input estimation for linear discrete-time systems," *Automatica*, vol. 42, no. 11, pp. 1883–1889, 2006.

[16] S. Gillijns and B. De Moor, "Unbiased minimum-variance input and state estimation for linear discrete-time systems with direct feedthrough," *Automatica*, vol. 43, no. 5, pp. 111–116, 2007.

[17] H. J. Palanthandalam-Madapusi and D. S. Bernstein, "Unbiased Minimum-Variance Filtering for Input Reconstruction," in *Proc. Amer. Control Conf.*, 2007, pp. 11–13.

[18] C.-C. Ho and C.-K. Ma, "Active vibration control of structural systems by a combination of the linear quadratic Gaussian and input estimation approaches," *J. Sound Vibrat.*, vol. 301, nos. 3–5, pp. 429–449, 2007.

[19] C.-S. Hsieh, "Extension of unbiased minimum-variance input and state estimation for systems with unknown inputs," *Automatica*, vol. 45, no. 9, pp. 2149–2153, 2009.

[20] H. Khaloozadeh and A. Karsaz, "Modified input estimation technique for tracking manoeuvring targets," *IET Radar, Sonar Navigat.*, vol. 3, no. 1, pp. 30–41, Feb. 2009.

[21] R. Orjuela, B. Marx, J. Ragot, and D. Maquin, "On the simultaneous state and unknown input estimation of complex systems via a multiple model strategy," *IET Control Theory Appl.*, vol. 3, no. 7, pp. 877–890, Jul. 2009.

[22] H. Palanthandalam-Madapusi and D. S. Bernstein, "A subspace algorithm for simultaneous identification and input reconstruction," *Int. J. Adapt. Control Signal Process.*, vol. 23, pp. 1053–1069, Dec. 2009.

[23] M.-S. Chen and C.-C. Chen, "Unknown input observer for linear non-minimum phase systems," *J. Franklin Inst.*, vol. 347, no. 2, pp. 577–588, 2010.

[24] S. Kirtikar, H. Palanthandalam-Madapusi, E. Zattoni, and D. S. Bernstein, "l-delay input and initial-state reconstruction for discrete-time linear systems," *Circuit, Syst., Signal Process.*, vol. 30, no. 1, pp. 233–262, 2011.

[25] H. Fang, Y. Shi, and J. Yi, "On stable simultaneous input and state estimation for discrete-time linear systems," *Int. J. Adaptive Control Signal Process.*, vol. 25, no. 8, pp. 671–686, 2011.

[26] H. Fang, R. A. de Callafon, and J. Cortes, "Simultaneous input and state estimation for nonlinear systems with applications to flow field estimation," *Automatica*, vol. 49, no. 9, pp. 2805–2812, 2013.

[27] J. Yang, F. Zhu, and X. Sun, "State estimation and simultaneous unknown input and measurement noise reconstruction based on associated observers," *Int. J. Adaptive Control Signal Process.*, vol. 27, no. 10, pp. 846–858, 2013.

[28] J. Sanchez and H. Benaroya, "Review of force reconstruction techniques," *J. Sound Vibrat.*, vol. 333, no. 14, pp. 2999–3018, 2014.

[29] A. Termehchy and A. Afshar, "A novel design of unknown input observer for fault diagnosis in non-minimum phase systems," *IFAC Proc. Vols.*, vol. 47, no. 3, pp. 8552–8557, 2014.

[30] S. Z. Yong, M. Zhu, and E. Frazzoli, "A unified filter for simultaneous input and state estimation of linear discrete-time stochastic systems," *Automatica*, vol. 63, pp. 321–329, Jan. 2016.

[31] P. Lu, E.-J. van Kampen, C. C. de Visser, and Q. Chu, "Framework for state and unknown input estimation of linear time-varying systems," *Automatica*, vol. 73, pp. 145–154, Nov. 2016.

[32] A. Chakrabarty, R. Ayoub, S. H. Żak, and S. Sundaram, "Delayed unknown input observers for discrete-time linear systems with guaranteed performance," *Syst. Control Lett.*, vol. 103, pp. 9–15, May 2017.

[33] A. Ansari and D. S. Bernstein, "Adaptive input estimation for nonminimum-phase discrete-time systems," in *Proc. 55th IEEE Conf. Decision Control*, Dec. 2016, pp. 1159–1164.

[34] G. Marro and E. Zattoni, "Unknown-state, unknown-input reconstruction in discrete-time nonminimum-phase systems: Geometric methods," *Automatica*, vol. 46, no. 5, pp. 815–822, 2010.

[35] K. C. Veluvolu and Y. C. Soh, "High-gain observers with sliding mode for state and unknown input estimations," *IEEE Trans. Ind. Electron.*, vol. 56, no. 9, pp. 3386–3393, Sep. 2009.

[36] B. Xiao, S. Yin, and O. Kaynak, "Tracking control of robotic manipulators with uncertain kinematics and dynamics," *IEEE Trans. Ind. Electron.*, vol. 63, no. 10, pp. 6439–6449, Oct. 2016.

[37] B. Xiao and S. Yin, "Velocity-free fault-tolerant and uncertainty attenuation control for a class of nonlinear systems," *IEEE Trans. Ind. Electron.*, vol. 63, no. 7, pp. 4400–4411, Jul. 2016.

[38] A. M. D'Amato and D. S. Bernstein, "Adaptive forward-propagating input reconstruction for nonminimum-phase systems," in *Proc. Amer. Conf. Control*, 2012, pp. 598–603.

[39] R. Gupta, A. M. D'Amato, A. A. Ali, and D. S. Bernstein, "Retrospective-cost-based adaptive state estimation and input reconstruction for a maneuvering aircraft with unknown acceleration," in *Proc. AIAA Guid. Nav. Control Conf.*, Minneapolis, MN, USA, Aug. 2012.
[40] A. A. Ali, A. Goel, A. J. Ridley, and D. S. Bernstein, "Retrospective-cost-based adaptive input and state estimation for the ionosphere–thermosphere," *J. Aerosp. Inf. Syst.*, vol. 12, no. 12, pp. 767–783, 2015.
[41] L. Han, Z. Ren, and D. S. Bernstein, "Maneuvering target tracking using retrospective-cost input estimation," *IEEE Trans. Aerosp. Electron. Syst.*, vol. 52, no. 5, pp. 2495–2503, Oct. 2016.
[42] A. Ansari and D. S. Bernstein, "Aircraft sensor fault detection using state and input estimation," in *Proc. Amer. Control Conf.*, 2016, pp. 5951–5956.
[43] A. Ansari and D. S. Bernstein, "Estimation of angular velocity and rate-gyro noise for sensor health monitoring," in *Proc. Amer. Control Conf.*, 2017, pp. 128–133.
[44] Y. Rahman, A. Xie, J. B. Hoagg, and D. S. Bernstein, "A tutorial and overview of retrospective cost adaptive control," in *Proc. Amer. Control Conf.*, Boston, MA, USA, Jul. 2016, pp. 3386–3409.
[45] Y. Rahman, A. Xie, and D. S. Bernstein, "Retrospective cost adaptive control: Pole placement, frequency response, and connections with LQG control," *IEEE Control Syst.*, vol. 37, no. 5, pp. 28–69, Oct. 2017.
[46] Y. T. Chan, A. G. C. Hu, and J. B. Plant, "A Kalman filter based tracking scheme with input estimation," *IEEE Trans. Aerosp. Electron. Syst.*, vol. AES-15, no. 2, pp. 237–244, Mar. 1979.
[47] P. L. Bogler, "Tracking a maneuvering target using input estimation," *IEEE Trans. Aerosp. Electron. Syst.*, vol. AES-23, no. 3, pp. 298–310, May 1987.
[48] B. W. Ahn, J. W. Choi, T. H. Fang, and T. L. Song, "A modified variable dimension filter with input estimation for maneuvering target tracking," in *Proc. Amer. Control Conf.*, 2003, pp. 1266–1271.
[49] C. Yang and E. Blasch, "Characteristic errors of the IMM algorithm under three maneuver models for an accelerating target," in *Proc. 11th Int. Conf. Inf. Fusion*, Jun. 2008, pp. 1–8.
[50] X. R. Li and V. P. Jilkov, "Survey of maneuvering target tracking. Part II: Motion models of ballistic and space targets," *IEEE Trans. Aerosp. Electron. Syst.*, vol. 46, no. 1, pp. 96–119, Jan. 2010.
[51] Y. Wang, S. Sun, and L. Li, "Adaptively robust unscented Kalman filter for Tracking a Maneuvering Vehicle," *J. Guid. Control Dyn.*, vol. 37, no. 5, pp. 1696–1701, 2014.
[52] B. A. Francis and W. M. Wonham, "The internal model principle of control theory," *Automatica*, vol. 12, no. 5, pp. 457–465, Sep. 1976.

Ahmad Ansari received the B.S. degree in aerospace engineering from the Institute of Space Technology, Islamabad, Pakistan, in 2012, and the M.S. degrees in aerospace and electrical engineering from The University of Michigan, Ann Arbor, MI, USA, in 2015 and 2017, respectively, where he is currently pursuing the Ph.D. degree with the Aerospace Engineering Department.

His current research interests include adaptive control of aircraft as well as input estimation for sensor fault diagnostics.

Dennis S. Bernstein (F'81) received the B.Sc. degree in applied mathematics from Brown University, Providence, RI, USA, in 1977, and the Ph.D. degree in control engineering from The University of Michigan, Ann Arbor, MI, USA, in 1982.

He is currently a Professor with the Aerospace Engineering Department, The University of Michigan. He is the Author of the book *Scalar, Vector, and Matrix Mathematics* (Princeton University Press, Third Edition in 2018). His current research interests include identification, estimation, and control for aerospace applications.